The Temperature Dependent Drag Crisis on a Sphere in Flowing Helium II

Choi, Y.S., NHMFL/FAMU-FSU College of Engineering
Smith, M.R., NHMFL
Van Sciver, S.W., NHMFL/FAMU-FSU College of Engineering

We have measured the drag coefficient on the surface of a sphere for temperature between 1.6 K and 2.0 K in flowing He II. The experiment consists of a 10 mm diameter sphere suspended upon a strut, oriented perpendicular to the oncoming flow, which spans the tunnel. A single pressure tap located on the surface of the sphere is used to map out the pressure distribution on the azimuth connecting the upstream and downstream points by rotating the sphere. This pressure distribution is then integrated to yield the form drag.[1] Since many of the important dynamics are dependent upon the equatorial velocity (θ=90°), the Reynolds number is calculated based upon the mean velocity in this smallest cross-section.

In our measurements, the Reynolds number spans the range from about $1x10^5$ to $8x10^5$. Profiles for Reynolds number at or above $1.8x10^5$ show supercritical behavior with the boundary layer separation occurring at approximately 100°. The data corresponding to the two lowest Reynolds numbers exhibit variations, which may be due to transition, together with very low signal levels. Assuming azimuthal symmetry of the pressure distribution with respect to the oncoming flow, together with the spherical shape of the surface, we may integrate the coefficient of pressure to calculate the coefficient of drag directly.

Scaling the He II two fluid equations suggests that pressure profiles should depend on the normal fluid Reynolds number, $Re_n=\rho_n ud/\eta_n$. Although this is in conflict with pipe flow data, it suggests a temperature dependence to the drag coefficient, which can be studied by experiment. Fig. 1 is a plot of the measured drag coefficient for fixed Reynolds number.

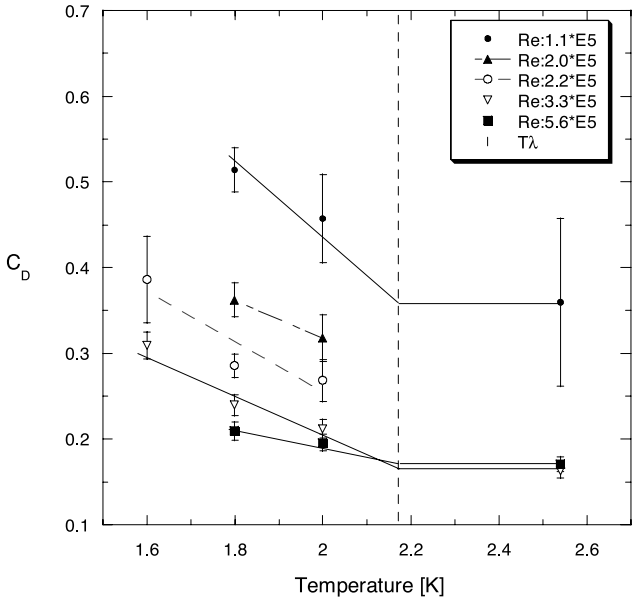

Figure 1. Drag coefficient vs. temperature.

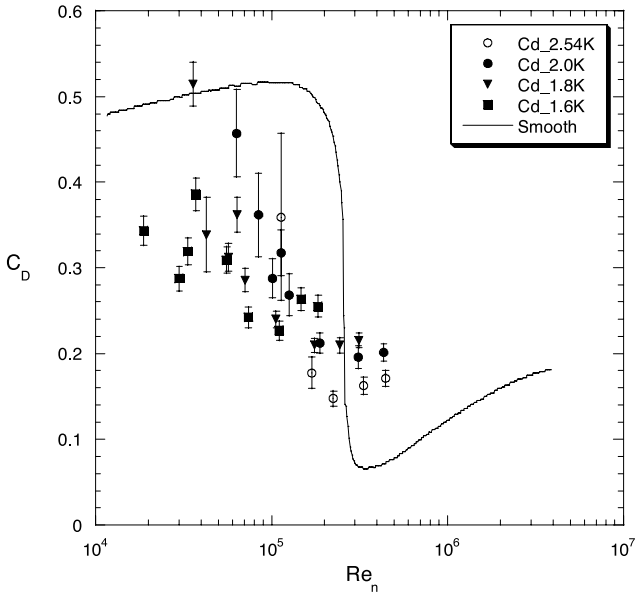

Figure 2. Drag coefficient vs. modified Reynolds number.

The coefficient is the largest at 1.6 K, decreasing monotonically to the relatively constant value in He I. Fig. 2 shows the drag coefficients vs. Re_n. The open symbols correspond to He I data and the closed symbols are for He II. The results also suggest that the drag coefficient in He II increases with decreasing temperature. Further, the minimum in the drag coefficient occurring just above the transition also increases with decreasing temperature. We note that the scaling shifts the minimum in the drag coefficient to approximately the same value of the

normal fluid Reynolds number for each temperature. That value, $Re_n \approx 2.3 \times 10^5$, is in reasonable agreement with the minimum in the classical drag coefficient curve at approximately $Re = 3 \times 10^5$. The variability in the He II data confirms a temperature dependence to the turbulent transition within boundary layer. Clearly, this topic needs further experiment supported by theoretical analysis.

Acknowledgements: This work supported in part by the Department of Energy, Division of High Energy Physics.

[1] Smith, M.R., *et al.,* Physics of Fluids, **11**, 4 (1999).
[2] Choi, Y.S., *et al.,* Proc. Workshop on Quantum Turbulence, Newton Institute, Cambridge, UK (2000).

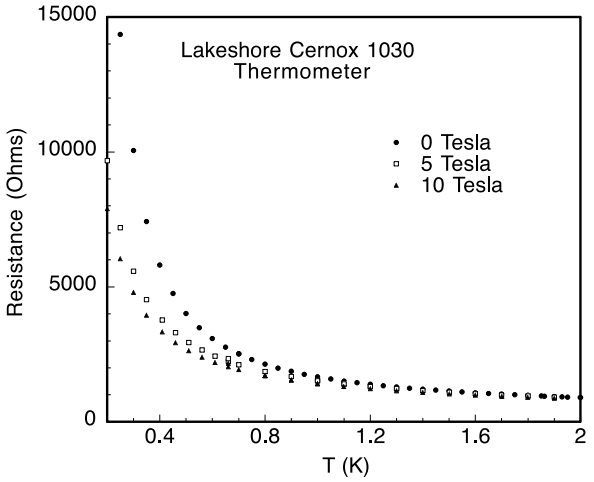

Figure 1. Resistance vs. temperature for a Lakeshore Cernox 1030 thermometer at 0, 5, and 10 T.

Magnetoresistance of Cernox Thermometers at High Fields

Freeman, E.J., Univ. of California, San Diego, Physics
Zapf, V.S., UC San Diego, Physics
Maple, M.B., UC San Diego, Physics

Low temperature thermometers, such as RuO and Cernox thin film chips, exhibit non-negligible magnetoresistance at temperatures below 1.8 K. Knowledge of this magnetoresistance is needed to accurately determine the temperature when measuring in a field. The NHMFL/Los Alamos 20 T magnet system is equipped with a specialized magnet system that compensates a region above the sample space to a negligible field. By thermally linking a temperature standard (in this case, a calibrated Cernox 1030 thermometer) in the compensated region to the sample space, we calibrated thermometers in fields from 0 to 10 T and temperatures from 200 mK to 2.5 K. In Fig. 1, we show the resistance vs. temperature characteristics for a Lakeshore Cernox 1030 thermometer at various fields. With the resistance as a function of field and temperature known for these thermometers, they can be used as standards to calibrate the magnetoresistance of other thermometers.

Pressure Drop and Heat Transfer in He II Forced Flow at High Reynolds Number

Fuzier, S., NHMFL/FAMU-FSU College of Engineering
Van Sciver, S.W., NHMFL/FAMU-FSU College of Engineering

An experiment to study forced flow of superfluid helium (He II) at high Reynolds number has been developed and successfully tested. This experiment is composed of a can/bellow assembly, which holds and generates the motion of the liquid through an experimental loop. This loop contains primarily a 1.2 m long 10 mm inside diameter straight stainless steal test section instrumented with thermometers, pressure transducers and a heater positioned in its middle. This experiment allows the study of fluid dynamics and heat transfer for Reynolds number up to $3*10^7$ in the test section.

The pressure drop is measured across a 1 m length part of the test section starting after the first 0.2m left for flow stabilization. It is converted into Fanning friction factors and shown in Fig. 2 (1m straight) with measurements from previous experiments of forced flow in pipes of various dimensions. These results are compared with two correlations for classical fluid turbulent flow. The Von Karman-Nikuradse smooth tube correlation

$$\frac{1}{\sqrt{f}} = 1.737\ln(\mathrm{Re}\sqrt{f}) - 0.396$$

typically used for Reynolds number less than $3*10^6$ and a correlation from Colebrook

$$\frac{1}{\sqrt{f}} = -4\log\left(\frac{\varepsilon}{3.7D} + \frac{1.25}{\mathrm{Re}\sqrt{f}}\right)$$

including the relative surface roughness

$\frac{\varepsilon}{D}$ ($\frac{\varepsilon}{D} = 1.4*10^{-4}$ for our experiment).

Our data are of the same order of magnitude but higher than this correlation. The difference is probably due at least in part to the presence of the thermometers positioned on the side of the test section in contact with the flow. We plan to do more measurements for a wider range of Reynolds number in the future.

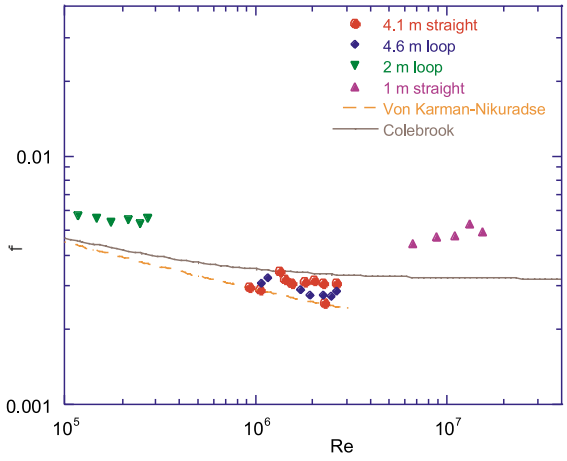

Figure 1. Friction factor for turbulent flow of He II for this and previous experiments.

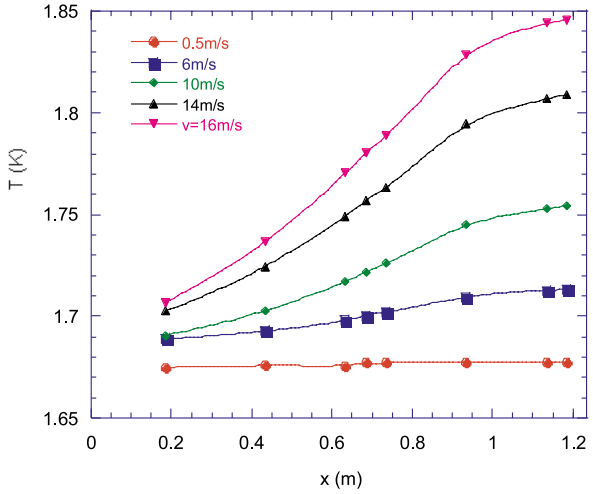

Figure 2. Joule-Thomson effect in forced flow He II (The lines are guides to the eyes).

Superfluid helium is warming during an isenthalpic expansion as the Joule-Thomson coefficient is negative for these low temperatures. This effect can have a noticeable influence on the design of large forced flow cooling systems and has to be taken into account in addition to regular heat transfer. We recorded the temperature profile along the test section for different flow velocities (Fig. 2). By construction, the temperature of the two extremities of this test section are close from the bath temperature of 1.657 K. The pressure drop along the pipe associated with the Reynolds number investigated is high enough to generate an observable temperature gradient.

Acknowledgments: This project is supported by the Department of Energy, Division of High Energy Physics, under grant FG02-96ER-40952.

Shock Pulses and Resonance Waves of Second Sound

Hilton, D.K., NHMFL/FSU, Physics
Van Sciver, S.W., NHMFL/FAMU-FSU College of Engineering

An instrumentation package to simultaneously detect second sound shock (SSS) pulses and induced quantum turbulence in He II is being developed. This system will be able to generate and detect SSS pulses in a channel of He II while monitoring for induced quantum turbulence at multiple points along the channel. The system will monitor for quantum turbulence by the attenuation of second sound resonance (SSR) waves. The experiments to be performed using this instrumentation package will offer the first opportunity to directly measure the quantum turbulence time and distance evolution of SSS pulses. These experiments have applications to transient heat transfer problems in He II, such as the cooling and stability of superconductors. The design and operation of thin-film thermometers and heaters for the detection and generation of SSS pulses and SSR waves is nearly finalized.

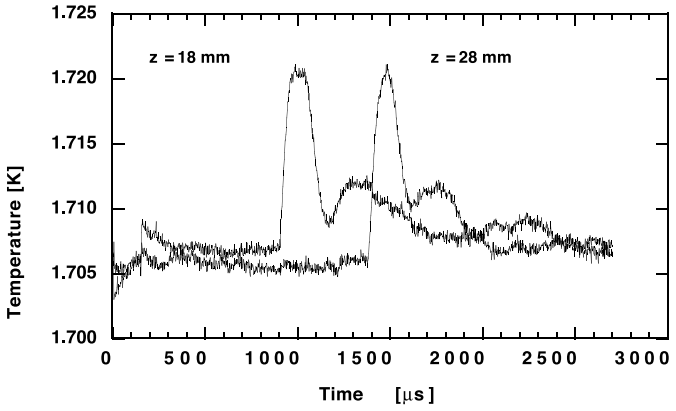

Figure 1. A plot of second sound shock (SSS) pulses from an initial square pulse of 20 W / cm^2 power flux density and 150 μs duration, in a He II bath at 1.7 K. The pulse propagation speed is 20.5 m / s.

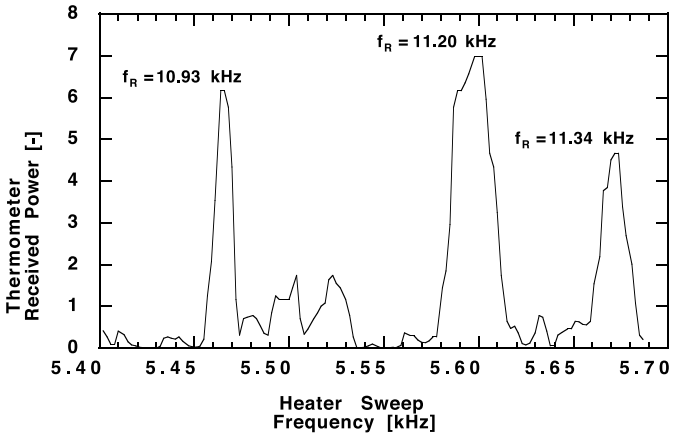

Figure 2. A plot of second sound resonance (SSR) peaks within a 42.6 mm long cylindrical cavity, in a He II bath at 1.76 K.

Shown in Fig. 1 are two samples of received SSS pulses. Each was generated within a cylindrical channel by a square pulse initiated at zero time into a He II bath at 1.7 K. Each trace is an average of 5 repeated measurements. The z values noted next to the pulses are the distances from the heater to the thermometer. Pulse propagation speed is 20.5 m/s, as measured by leading edge displacement, in agreement with tabulated second sound speeds and second sound theory. The baselines of the two traces correspond to the bath operating temperature at the times the traces were recorded.

Shown in Fig. 2 is a plot of received power versus sweep frequency, revealing SSR peaks. Sinusoidal rather than pulse power was delivered to the heater, and the frequency was linearly swept from the lower to the upper limits shown. The plot is a power spectrum of the cylindrical cavity. Each resonance frequency is the double of its corresponding sweep frequency because both, negative and positive halves of the electrical sinusoid delivered to the heater generate just positive thermal power in the He II bath. Each resonance frequency measured is within 1% of that calculated based on the experimental configuration and second sound theory. The three peaks shown correspond to three sequential normal modes of the cavity.

Acknowledgements: This research is supported by the U.S. Department of Energy Grant No. DE-FG02-96ER40751.

A Helium II Heat Transfer Level Meter

Zhang, T., NHMFL/FAMU-FSU College of Engineering
Smith, M.R., NHMFL
Van Sciver, S.W., NHMFL/FAMU-FSU College of Engineering

Liquid helium level meters are used for monitoring and controlling the liquid helium inside a cryogenics vessel. They are important for the operation of the cooling system in superconducting applications. In many of these applications, the coolant is superfluid helium (Helium II). He II has very high effective thermal conductivity and nearly constant density, which makes our design of He II heat transfer level meter possible.

Measurement Principle and Heat Transfer Analysis. The prototype level meter is a rectangular brass tube with height L=100 mm, width w=4.7 mm, depth d=2.3 mm, and wall thickness t=0.305 mm. Inside of the tube is full of liquid helium and contains a heater. During the measurement, the level meter will be immersed into a liquid helium reservoir whose level is to be measured. When the heater is turned on, heat will be transferred to the helium reservoir through four processes: (a) the Kapitza conductance

between the tube surface and liquid helium; (b) the free convection heat transfer between the helium vapor and brass tube; (c) the thermal conduction through the tube wall; and (d) axial conduction by fin effect. Based on the analysis and calculation, the free convection coefficient is two orders lower than the Kapitza conductance and thermal conductance, and can be neglected. The overall resistance R_{total} can be calculated by the law of series composite wall. The heat equation is,

$$Q = \frac{A \bullet \Delta T}{R_{total}} = \frac{P \bullet H \bullet \Delta T}{R_{total}} \qquad (1)$$

where R_{total} is a constant when the temperature is set and P is the perimeter of the brass tube and P=2(w+d)=14 mm. The above equation shows clearly the dependence of Q on H and ΔT, which is used to measure the liquid level.

Experimental Results and Discussions. Two kinds of measurements have been carried out using the prototype level meter. The first experiment is to keep the liquid level constant and verify the linear relationship between the heat power and temperature difference. The data confirm this relationship with a slight nonzero offset due to the residual heat leaked into the tube. The second experiment is to keep the temperature difference at constant. From Eq. (1), the heater power required to keep constant ΔT is proportional to the liquid level H. The experimental data shown in Fig. 1 verifies this point. That relationship is what we used to measure the liquid level.

An inherent limitation of the device, as configured, can be seen from the data in Fig. 1. During the experiment, the sensor was not stable and experienced thermal runaway for levels below 3 cm. This effect results from there being insufficient cooled surface to remove the heat deposited in the contained helium. In application, this limitation can be overcome by providing a small He II reservoir below the region where the level is to be measured. The small reservoir would stabilize the sensor and provide an offset so that it would operate in the linear region of heater power versus level.

Summary. A new measurement technique for liquid helium level has been developed. Complete analysis of heat transfer processes has been performed to predict the relation between the heat transfer rate and liquid level. The experimental results confirm that heat power is proportional to temperature difference at constant liquid level and proportional to liquid level at constant temperature difference. The data suggest the design of this level meter is reasonable and it can be applied in practical measurement.

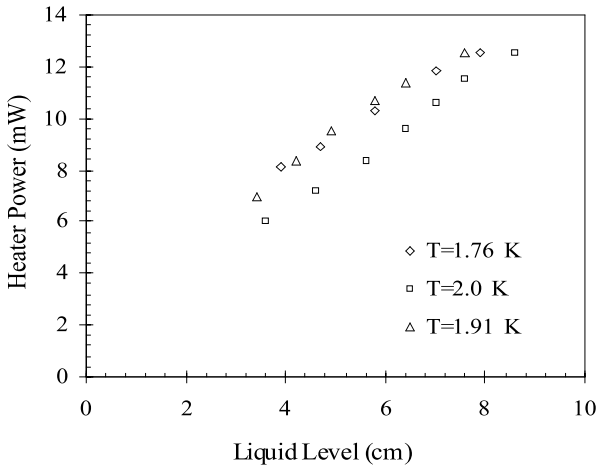

Figure 1. Heat power versus liquid level at constant temperature difference (T=1.76 K, ΔT=13 mK; T=1.91 K, ΔT=10 mK; T=2.0 K, ΔT=8 mK;)

Acknowledgements: This work was supported by the NSF-Chemical Transport and Thermal Processing Division under grant CTS-9806725. We would like to also thank David Basso and Scott Maier for assistance.

[1] Hilton, D.K., *et al.*, Cryogenics, **39**, 485-487 (1999).
[2] Snyder, N.S., Cryogenics, **10**, 89 (1970).
[3] Incropera, F.P., *et al.*, Fundamentals of Heat and Mass Transfer, 4th edition, John Wiley & Sons, New York (1996).